Supporting Information

Polynuclear iron(II)-aminotriazole spin-crossover complexes ("polymers") in solution

Irene Bräunlich[1], Antoni Sánchez-Ferrer[2], Matthias Bauer[3], Rahel Schepper[3], Philippe Knüsel[1], Julia Dshemuchadse[1], Raffaele Mezzenga[2], Walter Caseri[1]

[1]*Eidgenössische Technische Hochschule (ETH) Zürich, Department of Materials, Wolfgang-Pauli-Strasse 10, 8093 Zürich, Switzerland*

[2]*Eidgenössische Technische Hochschule (ETH) Zürich, Department of Health Sciences and Technology, Schmelzbergstrasse 9, 8092 Zürich, Switzerland*

[3]*Technische Universität Kaiserslautern, Fachbereich Chemie, Erwin-Schrödinger-Strasse, 67663 Kaiserslautern, Germany*

a)

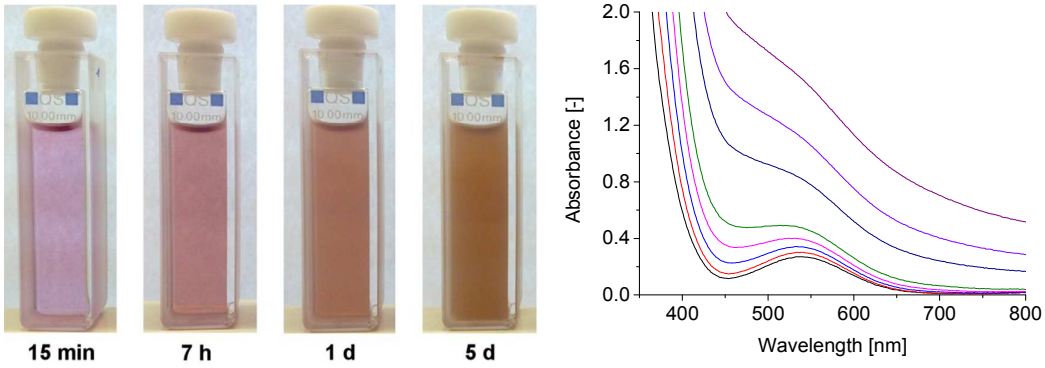

b)

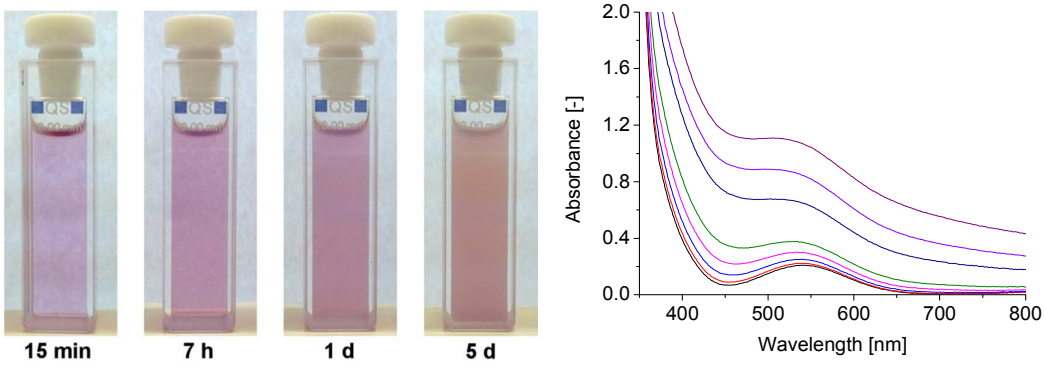

Figure SI-1: Solution of $[Fe(H_2O)_6](2ns)_2$ (0.0165 mol/L) and NH_2trz (NH_2trz/Fe^{2+} = 3:1) aged for 15 min, 1 h, 2 h, 4 h, 7 h, 1 d, 2 d and 5 d. a) Without ascorbic acid. b) With 33 % mol/mol ascorbic acid (with respect to iron). Left: Photographs. Right: UV/Vis absorption spectra (increasing aging from bottom to top).

Table SI-1: Bond distances in $[Fe(tpz)_2](2ns)_2 \cdot 2$ MeOH (between atom 1 and atom 2).

	Atom 1	Atom 2	Bond distance (Å)
$C_{20}H_{20}N_{12}Fe$	Fe1	– N1	1.9688(13)
	Fe1	– N1	1.9688(13)
	Fe1	– N2	1.9706(13)
	Fe1	– N2	1.9706(13)
	Fe1	– N3	1.9847(14)
	Fe1	– N3	1.9847(14)
	N1	– C1	1.330(2)
	N1	– N4	1.3626(18)
	N2	– C4	1.326(2)
	N2	– N5	1.3636(18)
	N3	– C7	1.327(2)
	N3	– N6	1.3675(18)
	N4	– C3	1.352(2)
	N4	– C10	1.443(2)
	N5	– C6	1.351(2)
	N5	– C10	1.445(2)
	N6	– C9	1.348(2)
	N6	– C10	1.441(2)
	C1	– C2	1.395(3)
	C2	– C3	1.365(3)
	C4	– C5	1.394(3)
	C5	– C6	1.362(3)
	C7	– C8	1.395(3)
	C8	– C9	1.358(3)
$C_{10}H_7O_3S$	S1	– O1	1.4467(19)
	S1	– O3	1.449(2)
	S1	– O2	1.4491(16)
	S1	– C11	1.7775(18)
	C11	– C20	1.366(3)
	C11	– C12	1.404(3)
	C12	– C13	1.361(3)
	C13	– C14	1.413(3)
	C14	– C19	1.416(3)
	C14	– C15	1.419(3)
	C15	– C16	1.362(3)
	C16	– C17	1.403(3)
	C17	– C18	1.363(3)
	C18	– C19	1.416(3)
	C19	– C20	1.418(3)
CH_3OH	O4	– C21	1.385(3)

Table SI-2: Bond angles in $[Fe(tpz)_2](2ns)_2 \cdot 2$ MeOH (atom 1 – atom 2 – atom 3).

$C_{20}H_{20}N_{12}Fe$

Atom 1	Atom 2	Atom 3	Bond angle (°)
N1	Fe1	N1	180.00(5)
N1	Fe1	N2	92.53(6)
N1	Fe1	N2	87.47(6)
N1	Fe1	N2	87.47(6)
N1	Fe1	N2	92.53(6)
N2	Fe1	N2	179.999(1)
N1	Fe1	N3	87.43(6)
N1	Fe1	N3	92.57(6)
N2	Fe1	N3	93.05(6)
N2	Fe1	N3	86.95(6)
N1	Fe1	N3	92.57(6)
N1	Fe1	N3	87.43(6)
N2	Fe1	N3	86.95(6)
N2	Fe1	N3	93.05(6)
N3	Fe1	N3	180
C1	N1	N4	104.97(13)
C1	N1	Fe1	136.68(12)
N4	N1	Fe1	118.31(10)
C4	N2	N5	105.34(13)
C4	N2	Fe1	136.07(12)
N5	N2	Fe1	118.19(10)
C7	N3	N6	104.44(13)
C7	N3	Fe1	137.30(12)
N6	N3	Fe1	118.20(10)
C3	N4	N1	111.57(14)
C3	N4	C10	129.97(14)
N1	N4	C10	118.34(13)
C6	N5	N2	111.19(14)
C6	N5	C10	130.19(14)
N2	N5	C10	118.36(12)
C9	N6	N3	111.65(14)
C9	N6	C10	130.49(14)
N3	N6	C10	117.86(13)
N1	C1	C2	110.86(16)
C3	C2	C1	105.94(16)
N4	C3	C2	106.65(15)
N2	C4	C5	110.60(16)
C6	C5	C4	106.09(16)
N5	C6	C5	106.77(15)
N3	C7	C8	111.24(16)
C9	C8	C7	105.76(16)
N6	C9	C8	106.92(16)
N6	C10	N4	109.60(13)
N6	C10	N5	109.37(13)

$C_{10}H_7O_3S$

N4	C10	N5	110.03(13)
O1	S1	O3	113.30(14)
O1	S1	O2	112.59(13)
O3	S1	O2	111.97(12)
O1	S1	C11	105.95(10)
O3	S1	C11	106.15(11)
O2	S1	C11	106.20(8)
C20	C11	C12	120.90(17)
C20	C11	S1	118.53(14)
C12	C11	S1	120.58(14)
C13	C12	C11	119.88(17)
C12	C13	C14	121.12(17)
C13	C14	C19	118.93(16)
C13	C14	C15	122.43(18)
C19	C14	C15	118.64(17)
C16	C15	C14	120.68(19)
C15	C16	C17	120.82(19)
C18	C17	C16	119.88(19)
C17	C18	C19	121.11(19)
C14	C19	C18	118.85(17)
C14	C19	C20	118.85(16)
C18	C19	C20	122.30(17)
C11	C20	C19	120.32(17)

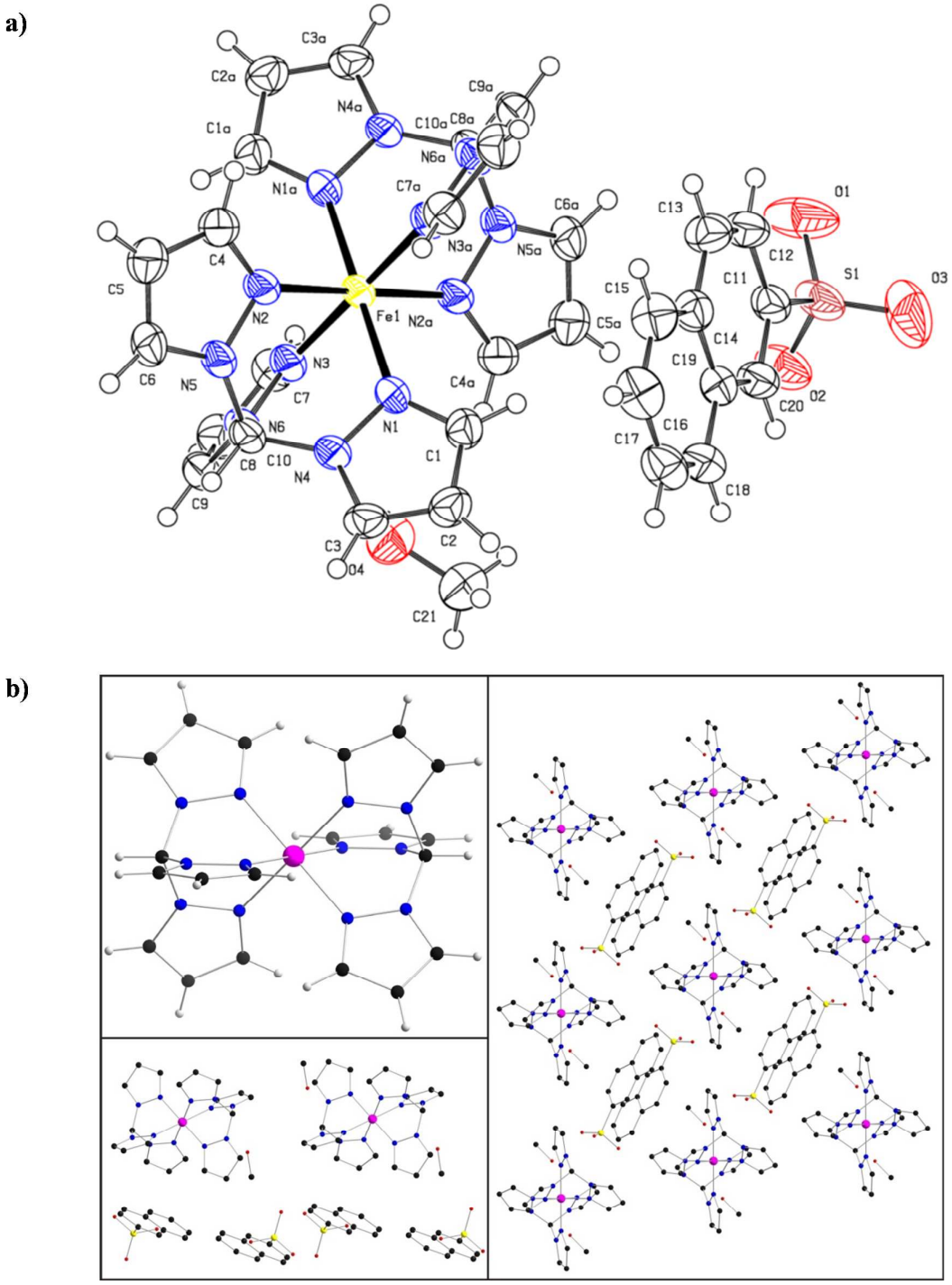

Figure SI-2: a) Representation of the $[Fe(tpz)_2](2ns)_2 \cdot 2$ MeOH structure. b) Top left: Structure of the $[Fe(tpz)_2]^{2+}$ ion. Bottom left: Line-up of the complex and the counter anions along the y-axis. Right: Structure in the x-z-plane. Hydrogen atoms are omitted in the latter two figures for simplicity.

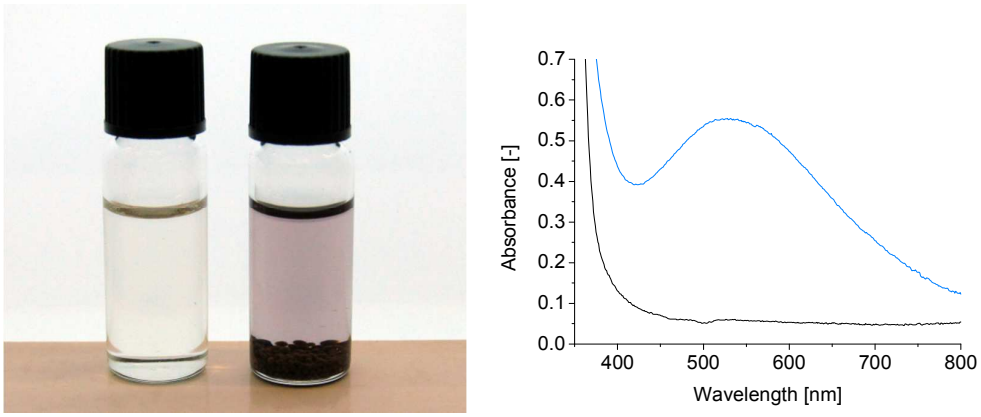

Figure SI-3: Solution of $[Fe(H_2O)_6](2ns)_2$ (0.0185 mol/L) and ascorbic acid (NH_2trz/Fe^{2+} = 6:1) in DMF. Photograph without molecular sieve (left vial) and with molecular sieve (3 Å, right vial). UV/Vis spectrum of solutions in DMF: dried with molecular sieve (3 Å, blue line) and without molecular sieve (black line).

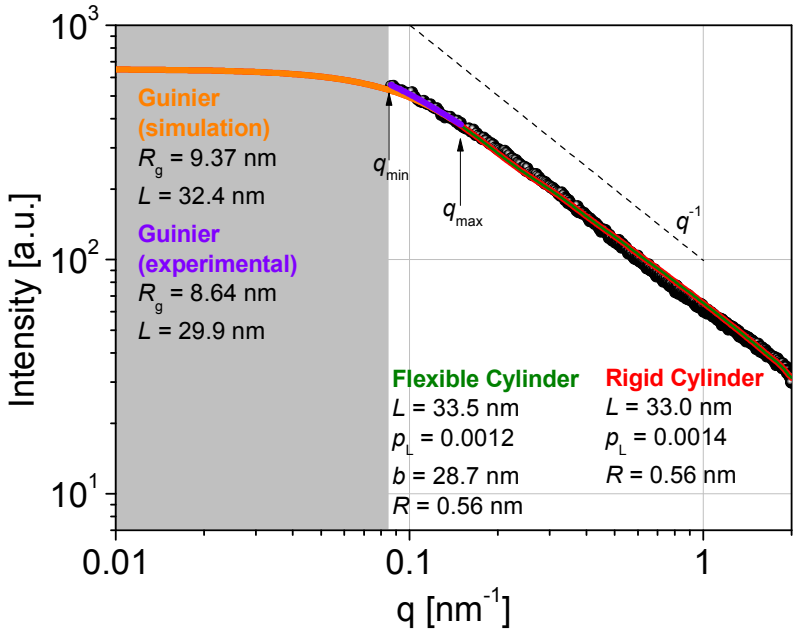

Figure SI-4: 1D radial scattering intensity distribution for molar NH_2trz/Fe^{2+} ratio of 9:1, at a total iron(II) concentration of 0.0185 mol·L^{-1} (black symbols). Simulated curves for the Flexible Cylinder model (green curve) and the Rigid Cylinder model (red curve) showing monodisperse contour length for the rigid polymer of L = 33.0 nm. Guinier regime from the simulated curves (orange curve), and from the experimental data (violet curve), with estimated radius of gyration of R_g (simulated) = 9.4 nm and R_g (experimental) = 8.6 nm and the corresponding polymer length of L (simulated) = 32.4 nm and L (experimental) = 29.9 nm.

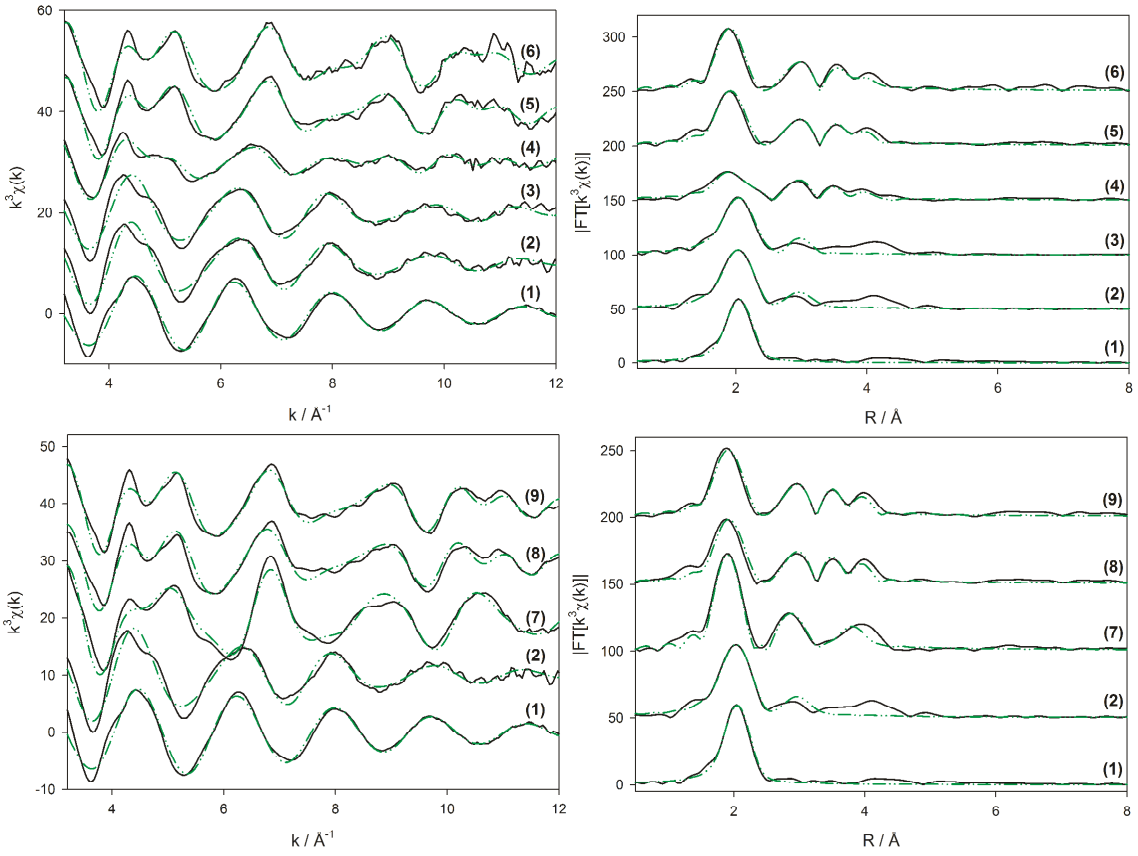

Figure SI-5: Experimental (black) and calculated (green) EXAFS spectra k3χ(k) (left) and the corresponding Fourier transformed functions (right) of samples in solution (top) and solid state (bottom). The labels of the spectra are included in Table 1.

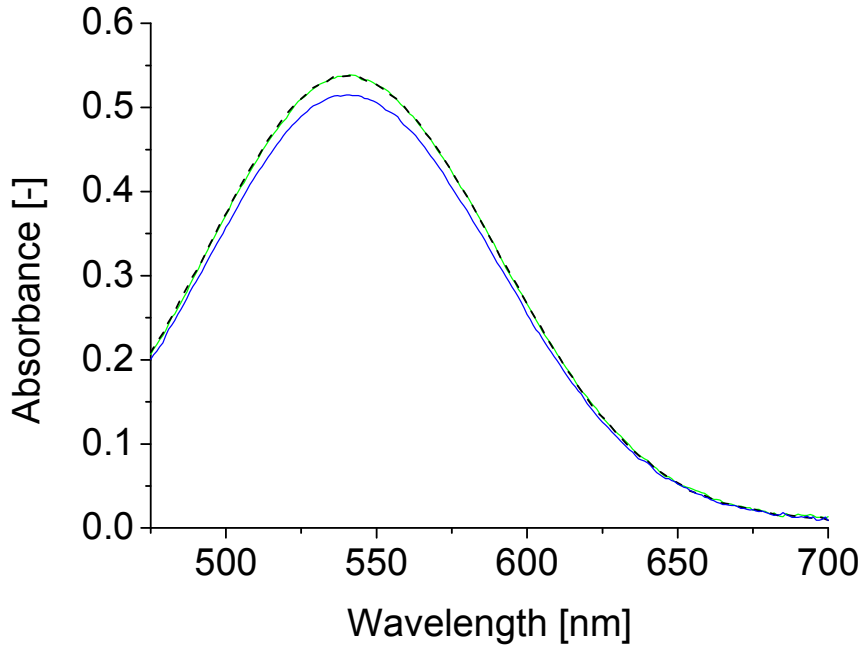

Figure SI-6: Vis absorption spectra 30 min after starting reactions of $[Fe(H_2O)_6](2ns)_2$ and NH_2trz in DMF. Black dashed line:Two-step reaction, initial concentration of Fe^{2+} 0.019 mol/L, NH_2trz/Fe^{2+} = 9:1. Addition of another 0.5 equivalents of Fe^{2+} after 15 min, final Fe^{2+} concentration: 0.018 mol/L, NH_2trz/Fe^{2+} = 6:1. Blue: Two-step reaction, initial concentration of Fe^{2+} 0.025 mol/L, NH_2trz/Fe^{2+} = 3:1. Addition of 3 molar equivalents of NH_2trz after 15 min, final Fe^{2+} concentration: 0.018 mol/L, NH_2trz/Fe^{2+} = 6. Green: One-step reaction, Fe^{2+} 0.018 mol/L, NH_2trz/Fe^{2+} = 6:1.

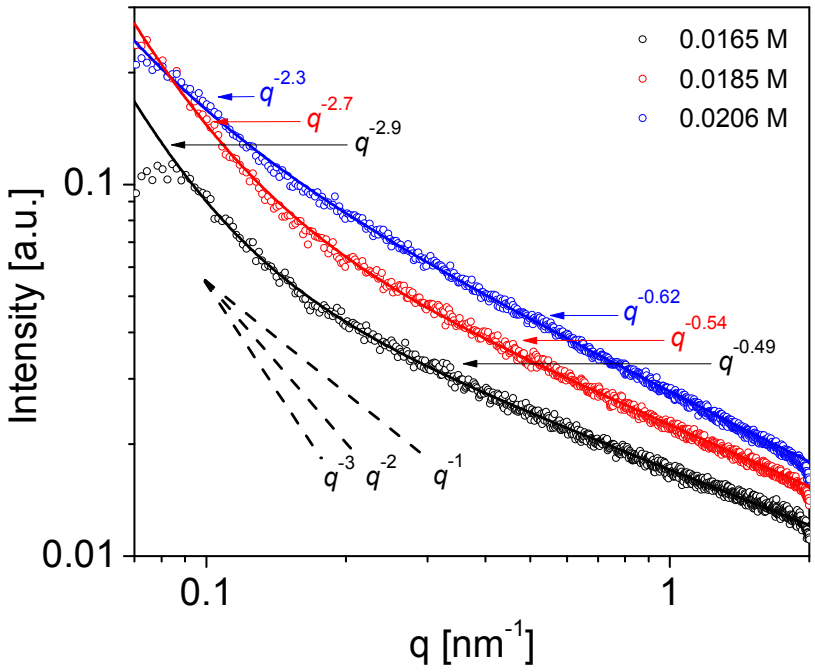

Figure SI-7: 1D radial scattering intensity distribution for three indicated total iron concentrations at the molar NH_2trz/Fe^{2+} ratio of 3:1, at 20 °C. The fitting curves show a fractal exponent at low-*q* values which indicates the presence of aggregates.

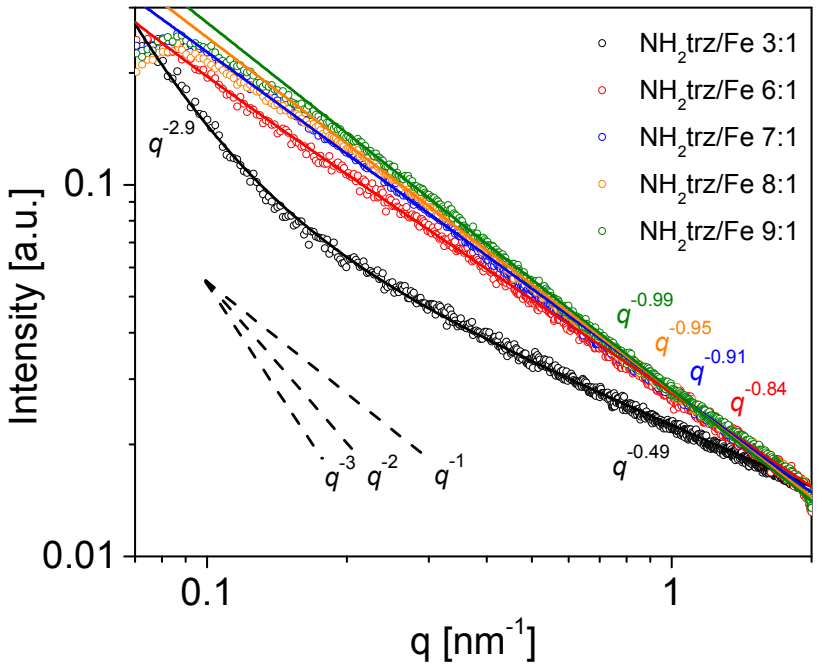

Figure SI-8: 1D radial scattering intensity distribution for five different stoichiometric ratios at total iron(II) concentration of 0.0185 M, at 20 °C. The fitting curve for the stoichiometric ratio of NH_2trz/Fe^{2+} of 3:1 shows a fractal exponent at low-q values which indicates the presence of aggregates.

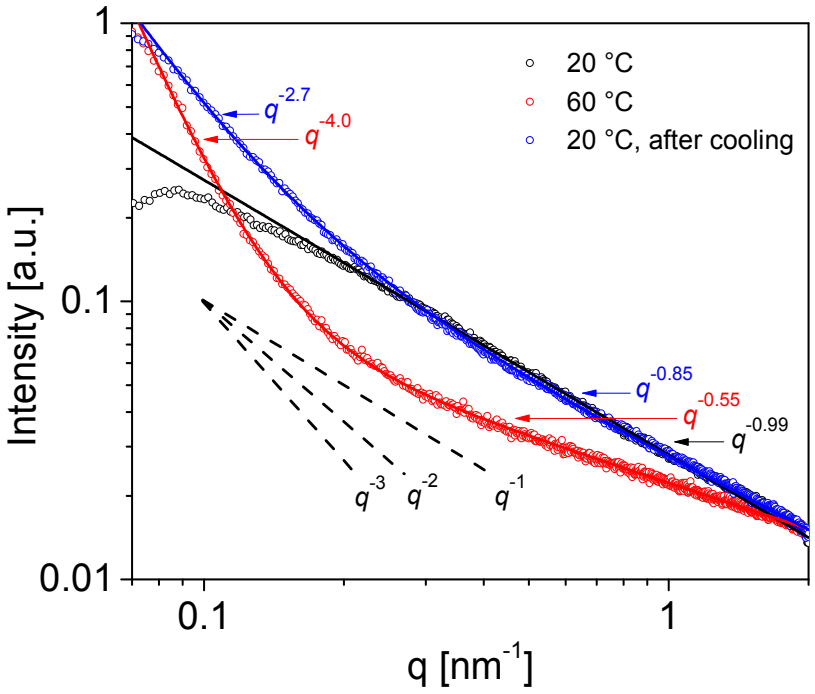

Figure SI-9: 1D radial scattering intensity distribution at different temperatures of a sample at a total iron(II) concentration of 0.0185 M and at a stoichiometric ratio of NH_2trz/Fe^{2+} of 9:1. The fitting curves at 60 °C and at 20 °C after cooling show a fractal exponent at low-*q* values which indicates the presence of aggregates.

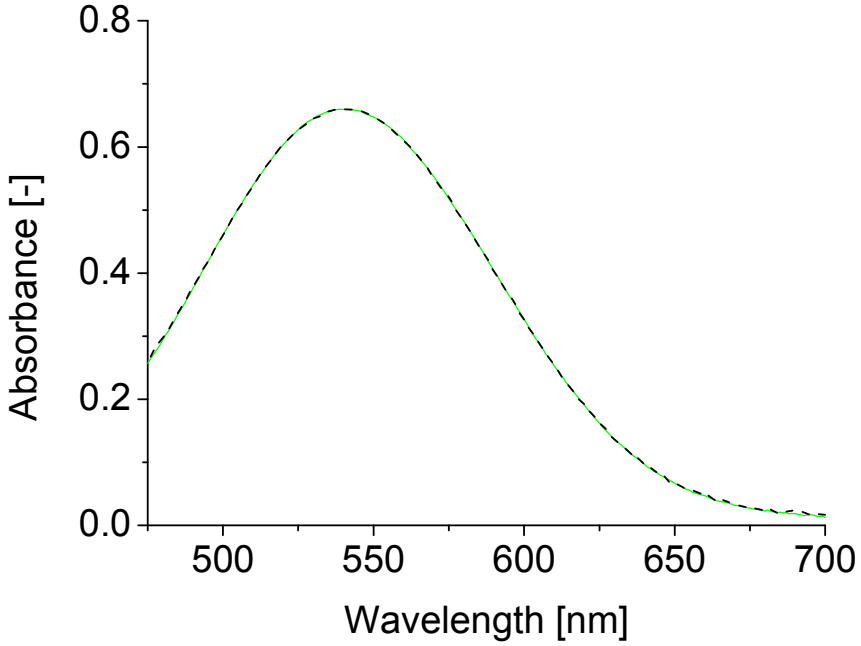

Figure SI-10: Vis absorption spectra of samples at an Fe^{2+} concentration of 0.0185 M. Black dashed line: NH_2trz/Fe^{2+} = 15:1. Green line: NH_2trz/Fe^{2+} = 3:1, multiplied by a factor of 2.619 to visualize the virtually identical band shape at different metal-to-ligand ratios.